TECHNICAL REPORT RD-RE-87-5

JOINT TRANSFORM OPTICAL CORRELATION

Tracy D. Hudson
David J. Lanteigne
Don A. Gregory
James C. Kirsch
Research Directorate
Research, Development, and
Engineering Center

OCTOBER 1987

U.S. ARMY MISSILE COMMAND
Redstone Arsenal, Alabama 35898-5000

Approved for public release; distribution is unlimited.

DISPOSITION INSTRUCTIONS

DESTROY THIS REPORT WHEN IT IS NO LONGER NEEDED. DO NOT RETURN IT TO THE ORIGINATOR.

DISCLAIMER

THE FINDINGS IN THIS REPORT ARE NOT TO BE CONSTRUED AS AN OFFICIAL DEPARTMENT OF THE ARMY POSITION UNLESS SO DESIGNATED BY OTHER AUTHORIZED DOCUMENTS.

TRADE NAMES

USE OF TRADE NAMES OR MANUFACTURERS IN THIS REPORT DOES NOT CONSTITUTE AN OFFICIAL INDORSEMENT OR APPROVAL OF THE USE OF SUCH COMMERCIAL HARDWARE OR SOFTWARE.

REPORT DOCUMENTATION PAGE

Form Approved
OMB No 0704-0188
Exp. Date Jun 30, 1986

1a. REPORT SECURITY CLASSIFICATION UNCLASSIFIED	1b. RESTRICTIVE MARKINGS
2a. SECURITY CLASSIFICATION AUTHORITY	3. DISTRIBUTION/AVAILABILITY OF REPORT Approved for public release; Distribution is unlimited.
2b. DECLASSIFICATION/DOWNGRADING SCHEDULE	
4. PERFORMING ORGANIZATION REPORT NUMBER(S) TR-RD-RE-87-5	5. MONITORING ORGANIZATION REPORT NUMBER(S)
6a. NAME OF PERFORMING ORGANIZATION Research Directorate RD&E Center 6b. OFFICE SYMBOL (If applicable) AMSMI-RD-RE	7a. NAME OF MONITORING ORGANIZATION
6c. ADDRESS (City, State, and ZIP Code) Redstone Arsenal, AL 35898-5248	7b. ADDRESS (City, State, and ZIP Code)
8a. NAME OF FUNDING/SPONSORING ORGANIZATION 8b. OFFICE SYMBOL (If applicable)	9. PROCUREMENT INSTRUMENT IDENTIFICATION NUMBER
8c. ADDRESS (City, State, and ZIP Code)	10. SOURCE OF FUNDING NUMBERS PROGRAM ELEMENT NO. / PROJECT NO. / TASK NO. / WORK UNIT ACCESSION NO

11. TITLE (Include Security Classification)

JOINT TRANSFORM OPTICAL CORRELATION

12. PERSONAL AUTHOR(S)
Tracy D. Hudson, David J. Lanteigne, Don A. Gregory, James C. Kirsch

13a. TYPE OF REPORT	13b. TIME COVERED	14. DATE OF REPORT (Year, Month, Day)	15. PAGE COUNT
Final	FROM _____ TO _____	1987/October/26	35

16. SUPPLEMENTARY NOTATION

17. COSATI CODES			18. SUBJECT TERMS (Continue on reverse if necessary and identify by block number)
FIELD	GROUP	SUB-GROUP	Optical Correlation Matched Filtering Pattern Recognition

19. ABSTRACT (Continue on reverse if necessary and identify by block number)

A study of the characteristics of a joint Fourier transform correlation has been completed. The correlation's characteristics experimentally confirm that the joint transform correlator is a viable alternative to the classical Vander Lugt correlator for optical pattern recognition applications.

20. DISTRIBUTION/AVAILABILITY OF ABSTRACT ☐ UNCLASSIFIED/UNLIMITED ☒ SAME AS RPT. ☐ DTIC USERS	21 ABSTRACT SECURITY CLASSIFICATION UNCLASSIFIED
22a. NAME OF RESPONSIBLE INDIVIDUAL Tracy D. Hudson	22b TELEPHONE (Include Area Code) (205) 876-1687 22c OFFICE SYMBOL AMSMI-RD-RE

DD FORM 1473, 84 MAR 83 APR edition may be used until exhausted
All other editions are obsolete

TECHNICAL REPORT RD-RE-87-5

JOINT TRANSFORM OPTICAL CORRELATION

Tracy D. Hudson
David J. Lanteigne
Don A. Gregory
James C. Kirsch
Research Directorate
Research, Development, and Engineering Center

October 1987

TABLE OF CONTENTS

LIST OF FIGURES

I. INTRODUCTION

The most widely used coherent optical architecture in optical computing and optical pattern recognition is the classical or Vander Lugt matched filtering correlator.[1] The basic Vander Lugt arrangement, shown in Figure 1, requires the fabrication of a holographic matched filter. The input scene may be a transparency or some real-time spatial light modulator such as a Liquid Crystal Light Valve (LCLV)[2] or a Modified Liquid Crystal Television (MLCTV).[3,4] A lens performs the Fourier transform of this input scene which then interferes with a plane wave reference beam on a photographic recording medium such as Kodak 649F plates. The plate is then developed and reintroduced into the arrangement at its original position. With the reference beam obstructed, if the Fourier transform of the test image matches that of the holographic recording, then the reference beam is recreated along its original path. This recreated beam is focused into a small bright spot, known as the correlation of the two images, and can be viewed either with a vidicon or CCD array.

Two disadvantages arise from the above technique. First, the plate must be photographically processed, thereby not allowing the direct comparison of two images, a reference and input scene, in real-time. Secondly, after development of the plate, it must be reintroduced into the system at its original position of exposure. This alignment is extremely critical and cannot deviate by more than a few microns from its position when the exposure was made.[5]

A Joint Transform Correlator (JTC)[6,7] architecture has recently received considerable attention as an alternative to the classical Vander Lugt arrangement because of its potential to overcome the above mentioned disadvantages of Vander Lugt filtering. The following advantages have been proposed by Yu and Ludman[8] using a magneto-optic spatial light modulator as the input device to a JTC arrangement: (1) large space-bandwidth product, (2) capability of performing multi-image cross correlation in real-time, and (3) high optical resolution.

This report contains the results of an in-depth study of the use of a JTC for pattern recognition. First, an introduction to the operation of a JTC is provided. Thereafter, the correlations obtained using a transparency as the input and reference scenes, coupled with a photographic plate (Kodak 649F) as the square-law fringe detector, are compared to a typical Vander Lugt correlation. As a practical matter, the transparency scenes were then replaced with a real-time modulator; specifically, a Litton Data Systems Magneto-Optic Spatial Light Modulator (MOSLM). The results of the MOSLM, operated in both amplitude and phase modes in a JTC, while still using the photographic plates as the square-law detector, will be discussed. This report also takes a brief look at using a LCLV as the square-law detector for dynamic correlating applications.

II. THE OPERATION OF A JOINT TRANSFORM CORRELATOR

The schematic representation of a joint transform correlator is shown in Figure 2. The input and reference scene transparencies are placed vertically in plane P_1 and illuminated with a collimated HeNe laser. The laser beam

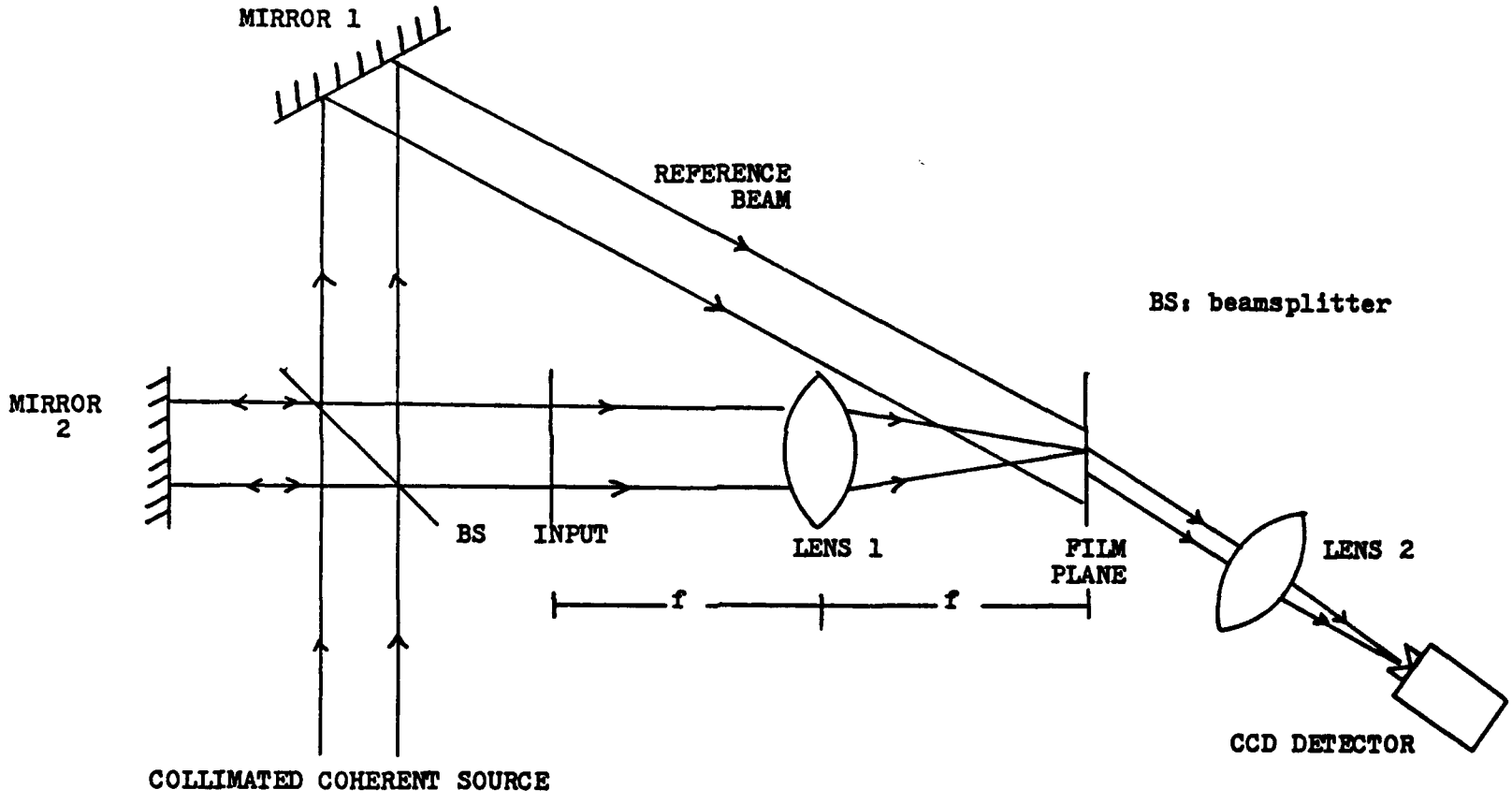

Figure 1. The Vander Lugt matched filter architecture.

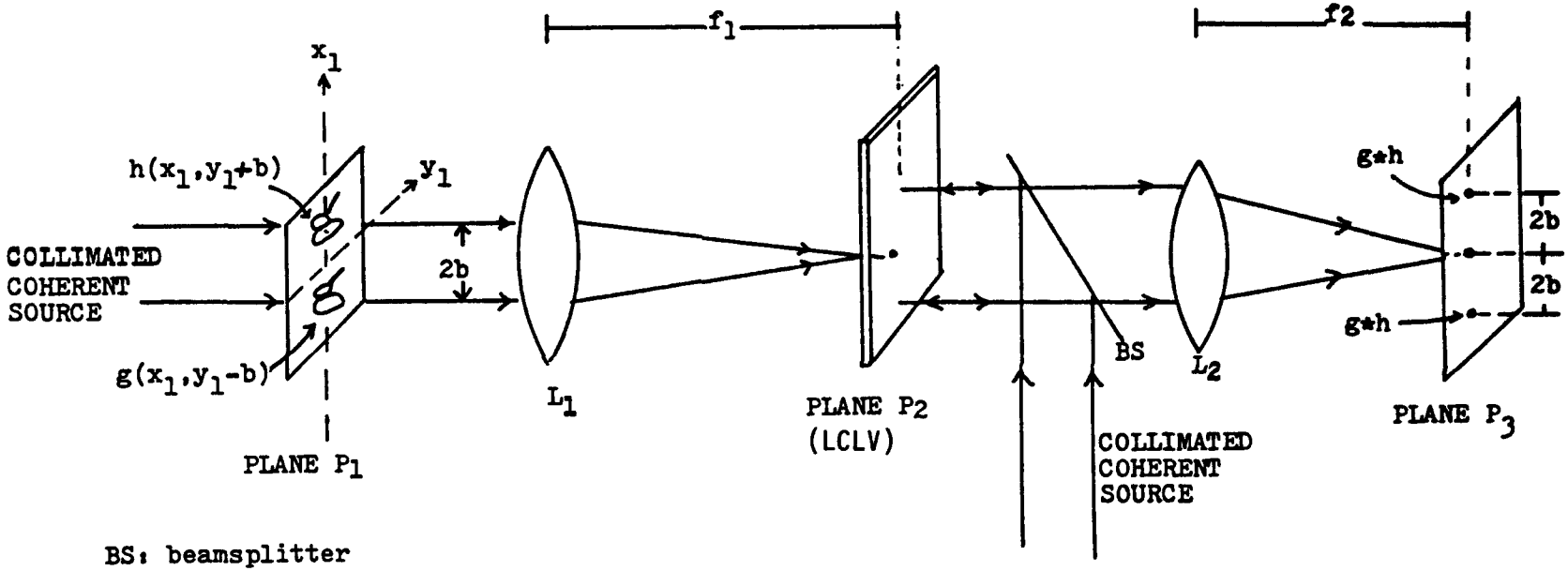

Figure 2. Schematic representation of a joint transform correlator.

containing the superimposed images is then Fourier transformed by lens L_1 and a square-law detector such as a LCLV is introduced in the back focal plane P_2. It is this property of simultaneously Fourier transforming the input and reference images with lens L_1 and the ensuing interference between the transforms of the two that enables one to cross-correlate spatial functions in real-time without photographic processing.[9] An important way of describing the quality of interference fringes is by their visibility. Ingwall and Fielding[10] states that the fringe visibility is calculated by the beam irradiance ratio $K = I_{ref}/I_{obj}$ with the equation

$$V = 2\sqrt{K} / (1+K). \tag{1}$$

The K ratio of a JTC is unity since the same collimated beam is used to illuminate and interfere the two input images. Therefore, the fringes have a visibility of unity. Furthermore, since the two images are transformed with the same lens, they may be positioned anywhere along the optical axis between lens L_1 and plane P_2 so long as the two images remain coplanar. The only change will be a variation in the scale of the resulting correlation.[11]

As stated by Casasent,[12] the amplitude transmittance of plane P_1 can be described by

$$U_1(x_1,y_1) = g(x_1,y_1 - b) + h(x_1,y_1 + b) \tag{2}$$

and the amplitude distribution of the light incident on plane P_2 is simply the Fourier transform of Equation (2), or

$$G(u,v)\exp(-i2\pi vb) + H(u,v)\exp(+i2\pi b) \tag{3}$$

where u and v are spatial frequencies of the x and y coordinates. The modulus squared of the light distribution given in Equation (3) is recorded at P_2 and the subsequent amplitude distribution of plane P_2 is given by the transmission of the exposed plate or

$$t_2(u,v) = |G|^2 + |H|^2 + GH^*\exp(-i4\pi vb) + G^*H\exp(+4\pi vb) \tag{4}$$

From Equation (4) it can be seen that both complex and real terms are involved. To record this information requires a medium sensitive to both. Plane P_2 is then illuminated with a collimated HeNe beam and Fourier transformed by lens L_2. The resulting light distribution at P_3 is

$$U_3(x_3,y_3)=g*g + h*h + g*h^*\delta(x_3,y_3+2b) + h*g^*\delta(x_3,y_3-2b) \tag{5}$$

where * represents correlation and 2b is the center-to-center spacing of the two scenes located in plane P_1.

The joint transform at P_2 scales according to f_1, the focal length of lens L_1. The inverse transform at P_3 scales according to f_2, the focal length of lens L_2, and inversely proportional to the size of the joint transform at P_2. Therefore, plane P_3 contains the desired cross-correlation terms of g and h centered at $(0,\pm bf_2/f_1)$. Furthermore, from Equation (5) the auto-correlations of the functions g and h are shown to be centered on the optical axis.

The resolution requirements of the detector in plane P_2 are a critical consideration in the JTC architecture. The spatial frequency that must be sampled by this detector is proportional to the center-to-center spacing of the input images in plane P_1. The minimum resolution required is determined by

$$(\sin \theta)/\lambda \quad (\text{lp/mm}) \tag{6}$$

where λ is the illuminating wavelength or 0.6328 μm for HeNe and $\sin \theta \approx \theta_{rad}$ or $2b/f_1$. Intuitively, one may scale the focal length of the transforming lens L_1 to trade off resolution against field of view in plane P_1.[13] Casasent and Furman[14] stated that the resolution requirements for the detector at plane P_2 are at least as stringent, and in some cases more stringent, for a JTC arrangement than the matched filter recording of a Vander Lugt system. This constraint appears to be the chief reason that the JTC has not been utilized more often.

III. THE EXPERIMENTAL JOINT TRANSFORM CORRELATOR

The experimental arrangement to photographically record the interaction of the transforms of the two images is shown in Figure 3. A Spectra-Physics Model 124B Helium-Neon laser was used to make the required exposures. The input plane P_1 consisted of a transparency of two identical tanks with black backgrounds (see Fig. 4) which were observed to have a center-to-center spacing of ≈1.3 cm. The Fourier transform lens FTL_1 had a focal length of 1069 mm and a diameter of ≈101 mm. A Kodak 649F glass plate was exposed at the Fourier transform plane P_2 with the emulsion side facing toward the laser. After exposure, the plate was developed using standard techniques (D-19 developer, Kodak stop bath, and Aerofix fixer A).[15] Once developed, the plate was introduced into the arrangement shown in Figure 5. In this arrangement, the exposed area of the plate was illuminated with a collimated plane wave from a Spectra-Physics Model 124B HeNe laser and afterwards Fourier transformed by lens FTL_2. Initially, lens FTL_2 had a focal length of 1069 mm but was later changed to a lens with a focal length of 914 mm.

A bright DC area located on the optical axis was observed at the focal plane using the lens with a focal length of 1069 mm. After the introduction of an opaque DC filter block just before the focal plane, two bright spots symmetrically located above and below the DC area by ≈1.5 cm were observed. These spots represent the cross-correlation between the two tanks. A photograph of the correlation plane is shown in Figure 6.

The plate was removed from its stationary holder and rotated to test for the sensitivity of the correlation intensity to the plate orientation. The correlation spots rotated along with the plate and with no significant change in intensity. The plate was then reintroduced into the holder with its emulsion side facing away from the laser as opposed to the original orientation of facing the laser. Again, no significant change in the correlation intensity was noted.

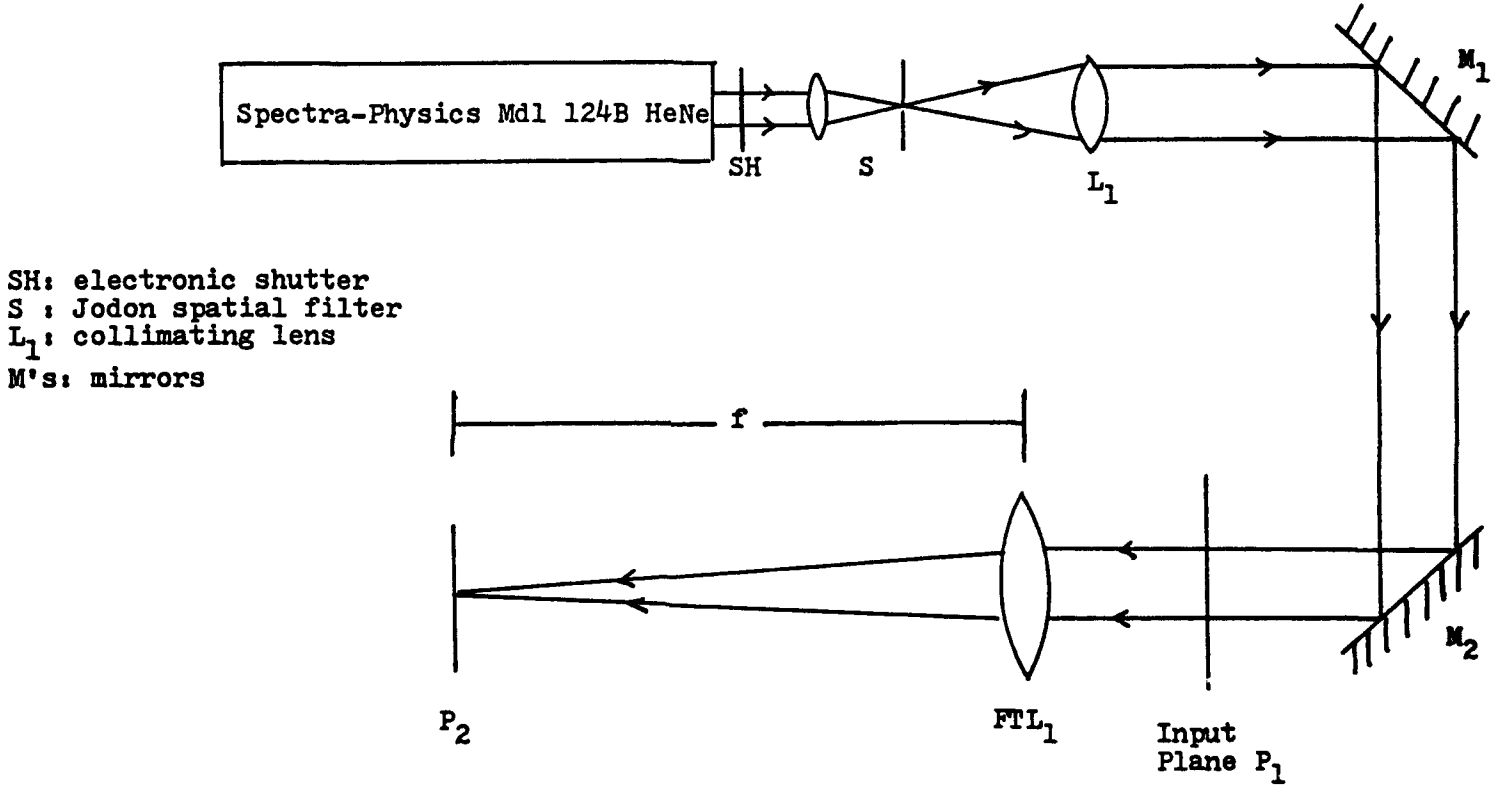

Figure 3. Experimental arrangement used to record the interference fringes.

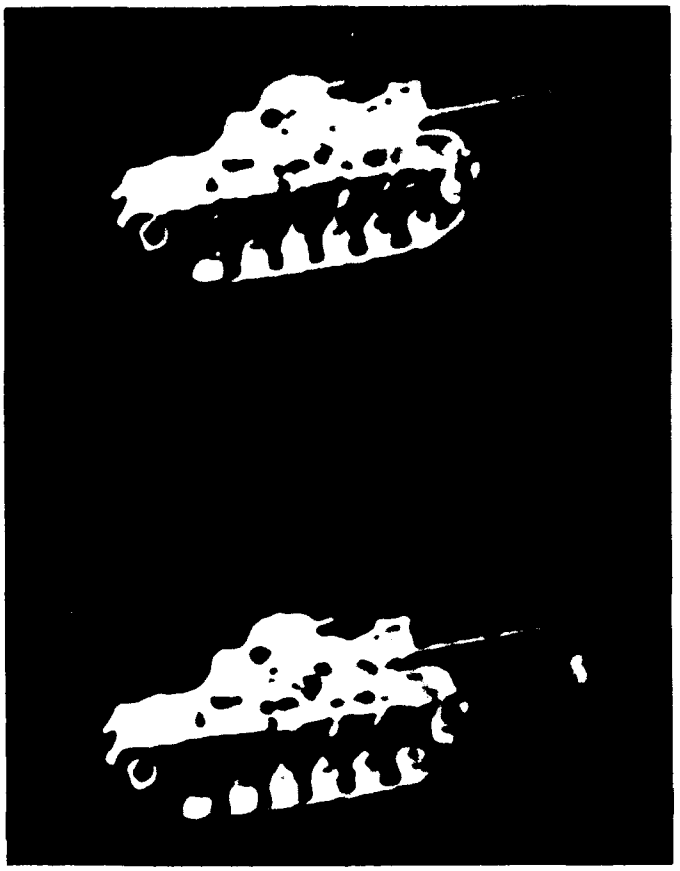

Figure 4. Enlarged photograph of the two tanks displayed on the input transparency.

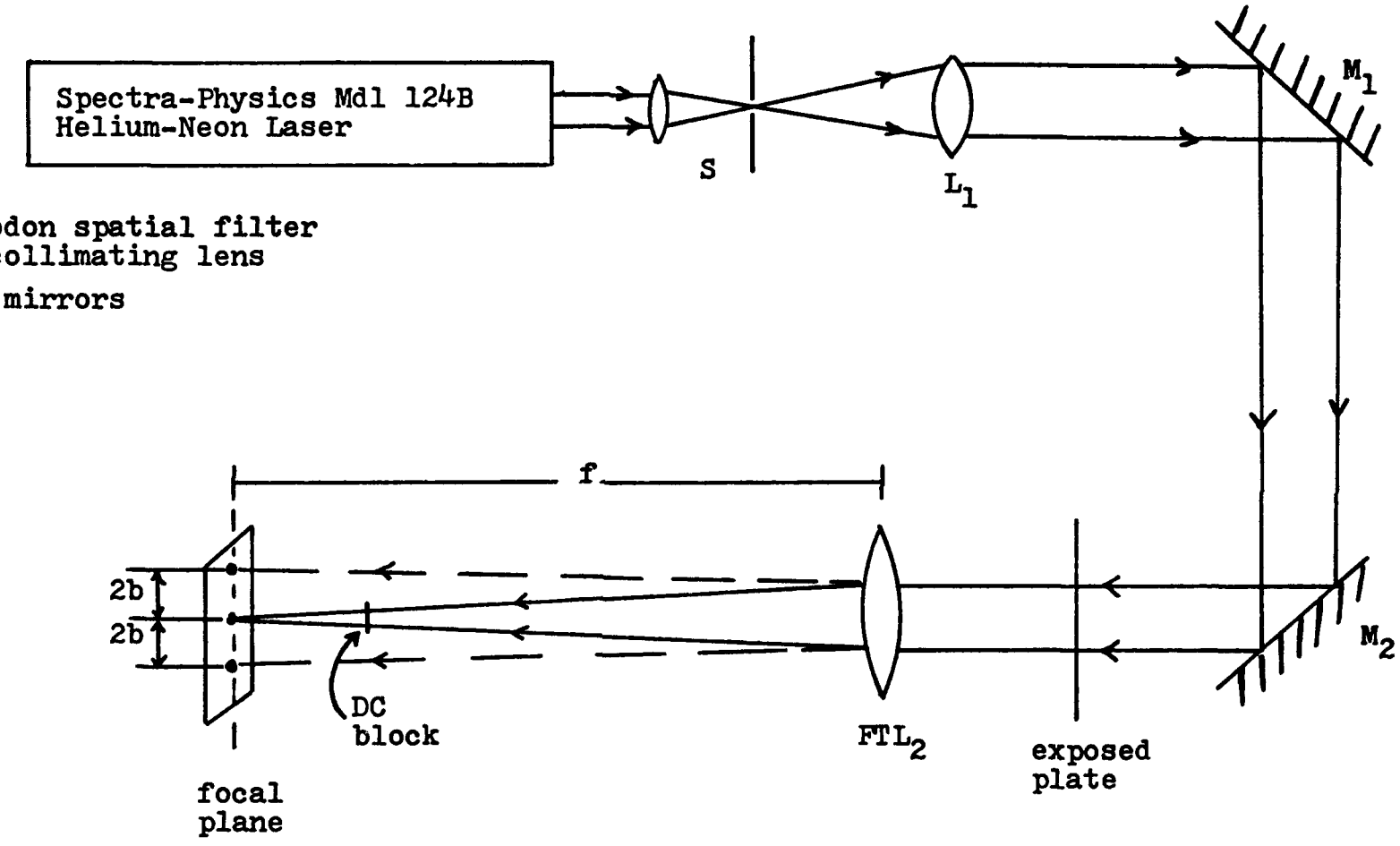

Figure 5. Experimental arrangement used to address the fringe structure recorded on the photographic plates.

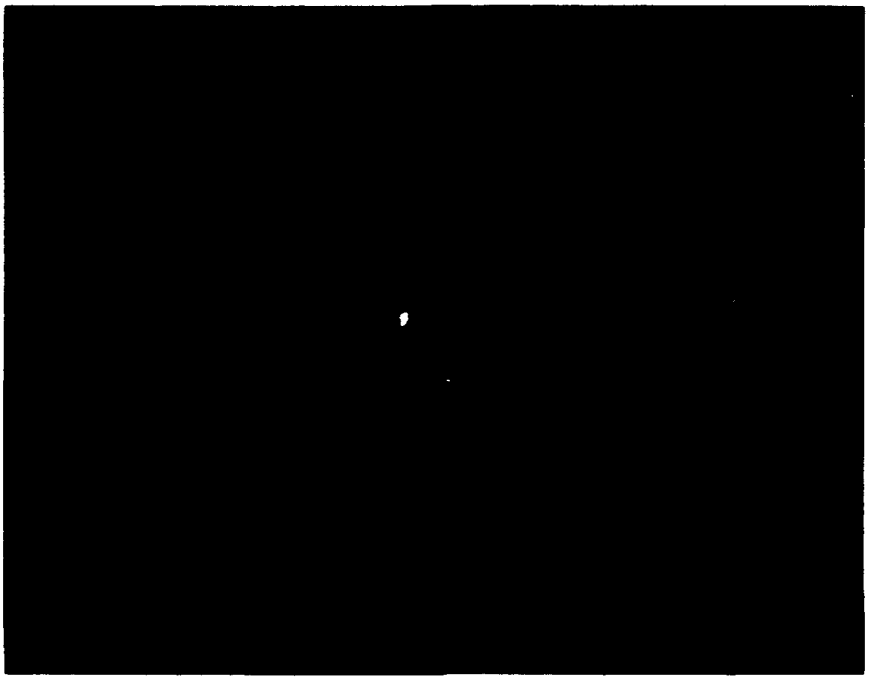

NOTE: The central order is the DC area which was partially blocked. The correlations are the bright areas directly above and below the DC area.

Figure 6. Photograph of the correlation plane using transparencies for the input images.

Next, a 30x microscope objective and vidicon imaging system was used to observe the structure of one of the cross-correlation terms. The correlation signal was composed of a central bright spot and three surrounding lobes. The amount of diffracted energy compared to the incident light on the plate was determined to be ≈2.8 percent for each cross-correlation term; or more concisely, 5.6 percent of the light incident on the plate was diffracted into the cross-correlation terms. An intensity scan of one of the correlations, shown in Figure 7, was performed using a Colorado Video Analyzer and a standard chart recorder. From Figure 7, the peak signal-to-peak noise of the upper correlation was determined to be 39:1 (15:91 dB). The peak signal-to-average noise is 195:1 (22.9 dB). The side lobes were not included in the signal-to-noise ratio calculations. The plate was then removed from the system and the interference fringes observed under a microscope. The fringes were measured to be 0.05 mm wide from center to center. Therefore, the square-law detector used must have a minimum resolution of 20 lp/mm. The fringe structure is shown in Figure 8.

Several more exposures were made utilizing the arrangement of Figure 3 so as to verify pattern discrimination and translational invariance of the correlator arrangement. At this point, the focal length of FTL_2 was changed to 914 mm. To verify the interference of the two transforms of the images, one of the tanks on the transparency was masked and an exposure was made. Once developed, the plate was introduced into the arrangement of Figure 5. No correlation intensities were detected in the focal plane; only the DC spot was evident. A micrograph of the exposed plate is shown in Figure 9. By comparison to the micrograph of Figure 8, one readily sees that no fringing has occurred in the latter exposure. One of the tanks was translated with respect to the other to verify translational invariance and again an exposure was performed. When introduced into the system of Figure 5, it was observed that the cross-correlation term above the DC area had translated directly proportional to the translation of the input images, and that the lower cross-correlation term had translated in the opposite direction of the input image translation. The peak signal-to-peak noise ratio of the translated correlation was 34.75:1 (15.41 dB) and the peak signal-to-average noise was 86.88:1 (19.39 dB). These signal-to-noise ratios are again neglecting the characteristic side lobes of the correlation signals. Furthermore, ≈2.2 percent of the incident energy on the plate was diffracted into each of the cross-correlation terms. The plate was examined under the microscope as before-fringing was evident. A photograph of the translated correlations is shown in Figure 10 and an intensity scan of the upper correlation is shown in Figure 11.

The JTC architecture employed in this investigation compares favorably to the classical Vander Lugt matched filtering architecture. The peak signal-to-peak noise ratios and the peak signal-to-average noise ratios are in the same range. However, the diffraction efficiency of a correlation from a JTC is 5 to 6 times greater than that of a classical matched filter correlation that also utilizes Kodak 649F plates as the recording medium. The JTC explored here exhibited a correlation efficiency of ≈2.8 percent whereas the typical Vander Lugt filter may exhibit an efficiency of ≈0.5 percent. Furthermore, the realignment of the plate into the system after exposure and development is much more straightforward in the JTC than in the Vander Lugt architecture where the matched filter must be realigned to

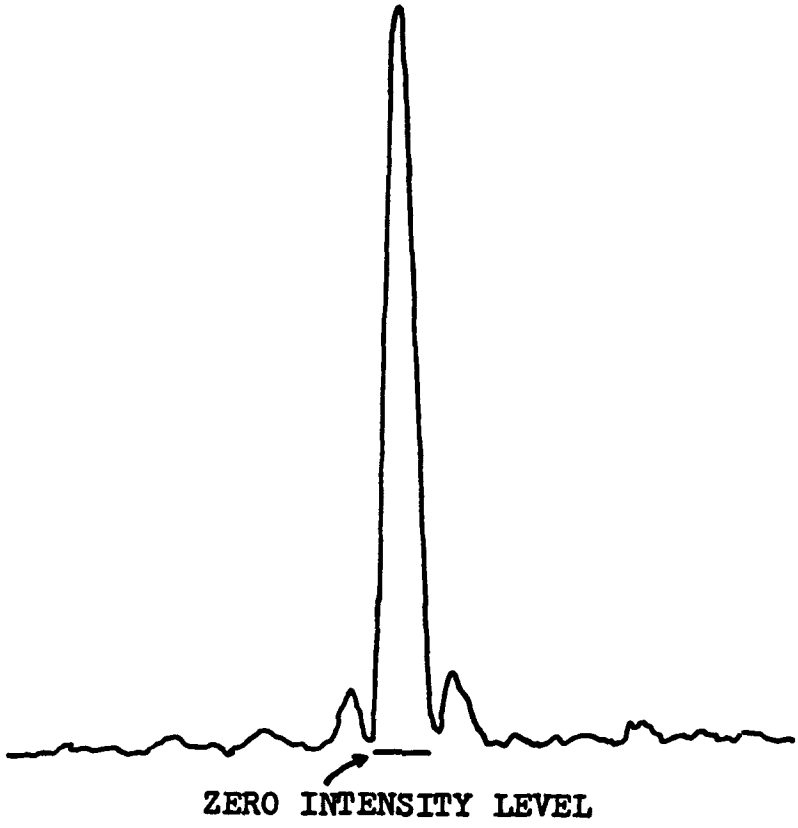

Figure 7. Trace of correlation intensity taken from video analyzer.

Figure 8. Fringe structure of the correlation recording shown in Figure 6 (50x magnification).

Figure 9. Micrograph of the recording of the Fourier transform of only one tank (50x magnification).

NOTE: No fringing is evident.

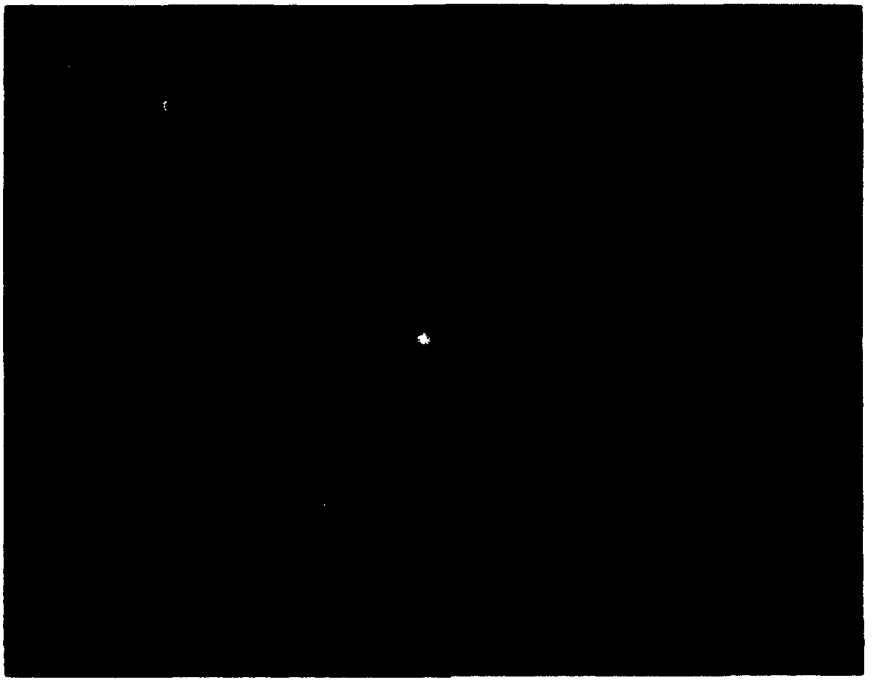

Figure 10. Photograph of the correlations due to one of the tanks on transparencies being translated with respect to the other.

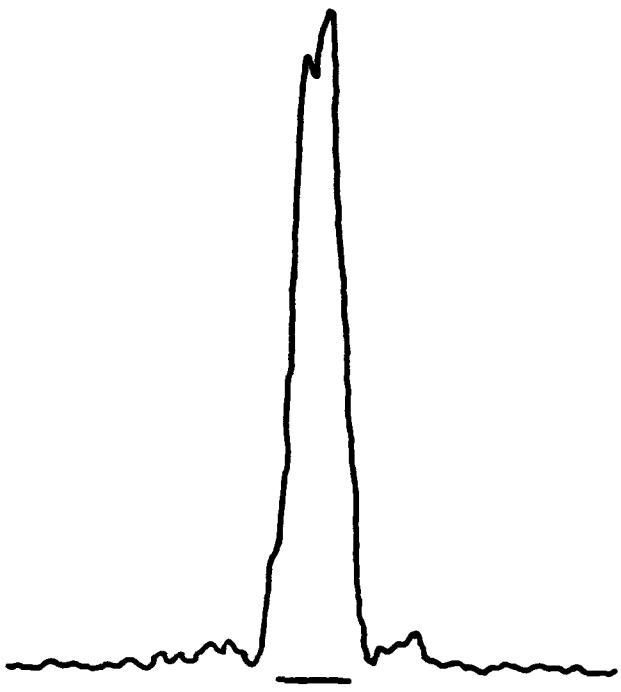

Figure 11. Trace of one of the translated correlations intensity taken from a video analyzer.

within a few microns of the original position. The fringe recording plate of a JTC can be positioned virtually anywhere within a plane wave beam.

IV. JOINT TRANSFORM CORRELATION USING A MAGNETO-OPTIC SPATIAL LIGHT MODULATOR

Real-time input scenes replaced the transparency inputs used above with the addition of a Magneto-Optic Spatial Light Modulator (MOSLM). The MOSLM is a partially transparent array of pixels on a semiconductor chip. Each pixel is made of a magnetic film that exhibits binary (left or right) Faraday rotation of polarized light. The polarity of each pixel can be controlled by means of currents driven through a grid of conductors surrounding the pixels, with the aid of an externally applied magnetic field.[16] After light goes through the device, it passes through a linear polarizer. If the polarizer is set so as to pass one polarization but not the other, an amplitude modulated image results. If the polarizer axis is set perpendicular to the incident polarized light, a phase modulated image results. The particular MOSLM used in this experiment was a 128 x 128 pixel device which had an effective surface area of approximately 1 cm^2. The experimental arrangement shown in Figure 12 was used to record the interference between the transforms of the input and reference scenes, using a Kodak 649F photographic plate. This arrangement was similar to that of Figure 3 except plane P_1 contained the MOSLM instead of transparencies, and a polarizer was used for amplitude or phase modulation of the input scenes. Furthermore, the focal length of FTL_1 was shortened to 254 mm in order to have approximately the same spacing between cross-correlation terms as before, since the input scenes were displayed simultaneously on the MOSLM and were thus closer together (center-to-center spacing of $\approx$0.3 cm).

The first exposures performed with the arrangement of Figure 12 were with the MOSLM being amplitude modulated. Examples of the binary images displayed on the device are shown in Figures 13 through 15. First, two identical tanks (Fig. 13) were written to the device and exposures of their transform interactions were recorded on photographic plates. The developed plates were then addressed using the system shown in Figure 5. The cross-correlation terms were present in the transform plane; however, these terms were not as pronounced as those discussed in Section III of this report. No accurate signal-to-noise ratios were calculated, but they were marginal at best. Furthermore, only 0.1 percent of the energy which was incident on the plate was actually diffracted into each of the cross-correlation terms. The plate was removed from the system and observed for fringing under a microscope. The fringing was present but not as pronounced as the fringing observed when the transparencies were utilized. Photographs of the correlations and the fringe structure are shown in Figures 16 and 17.

Next, a new pattern was written to the MOSLM. This pattern was that of two tanks identical in nature except for the fact that one was translated with respect to the other (Fig. 14). This image was used to verify the translational invariance of the correlator as discussed in Section III. An exposure identical to the one above was taken, and after development, was addressed with the same system used previously. The correlation signals were present and translated as expected. Again, these signals were surrounded by noise and no accurate signal-to-noise ratios were measured. Also, only

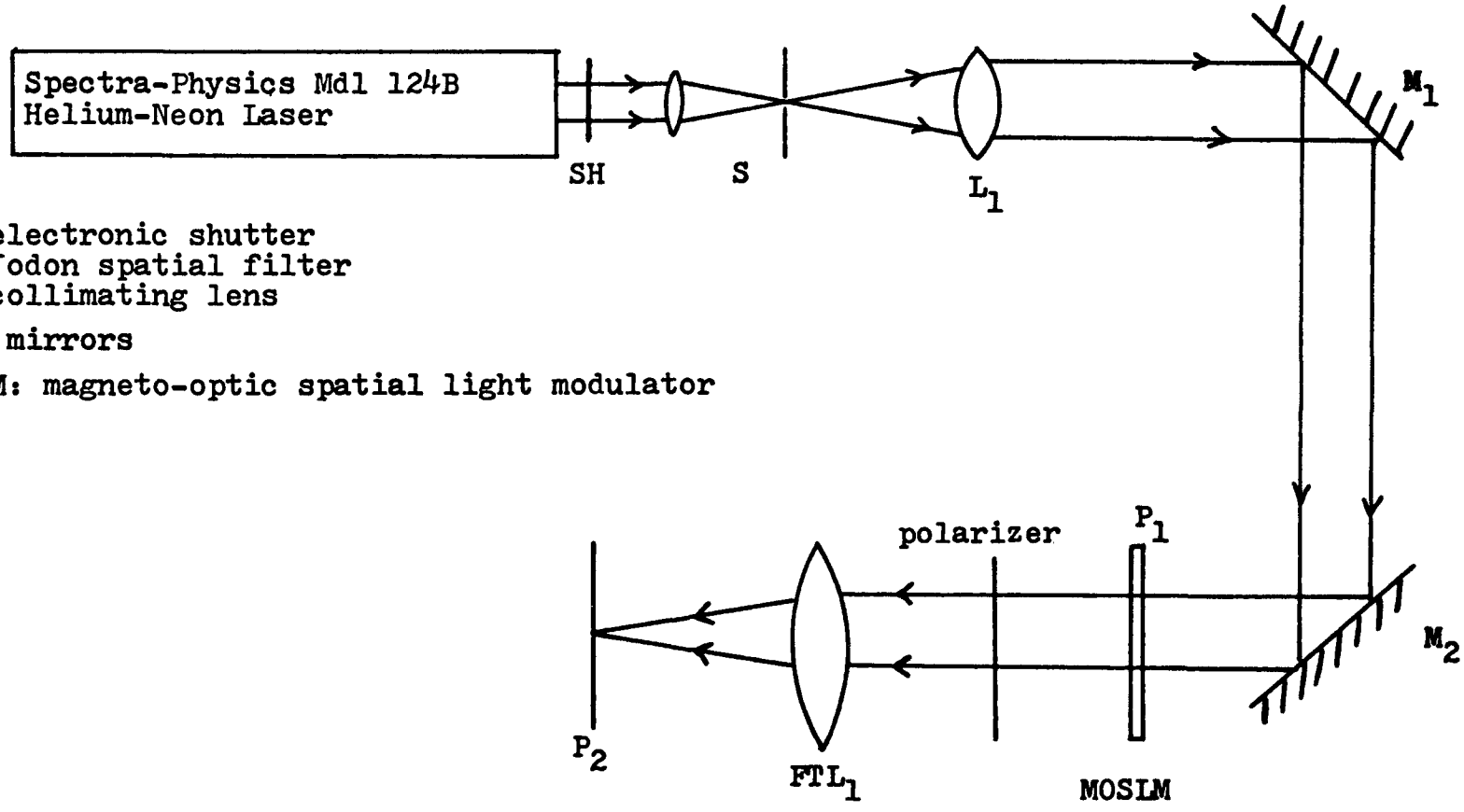

Figure 12. Experimental arrangement to record the fringe structure from images displayed on MOSLM.

Figure 13. Two identical tanks displayed on the MOSLM.

Figure 14. Two tanks, one translated with respect to the other, displayed on the MOSLM.

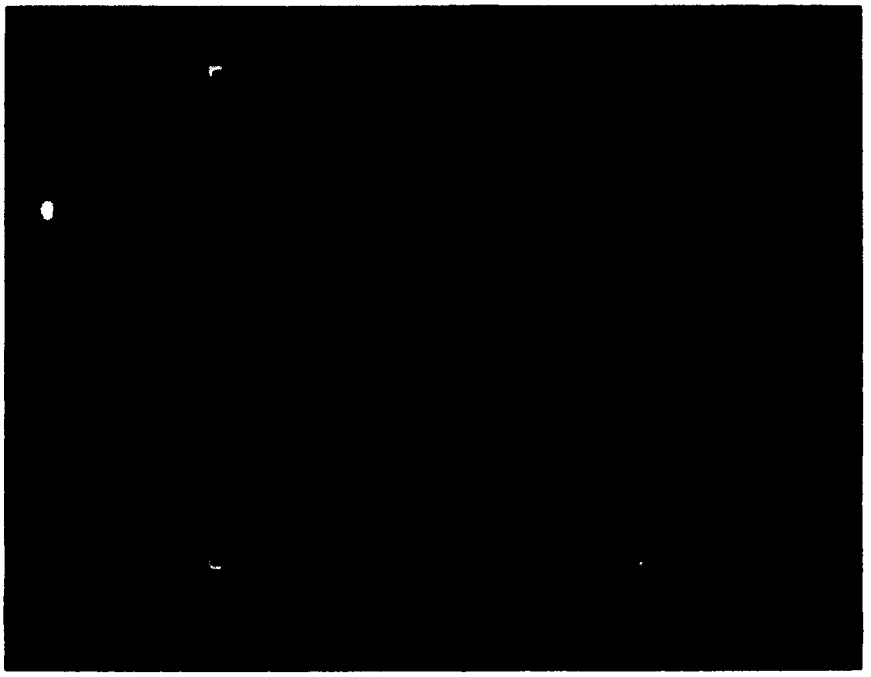

Figure 15. Two tanks, one rotated with respect to the other, displayed on the MOSLM.

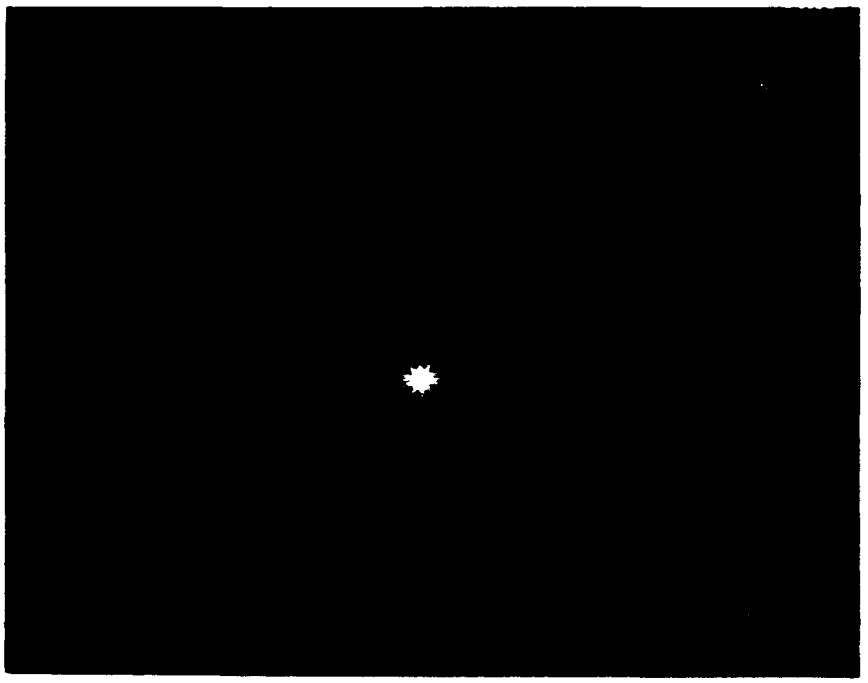

Figure 16. Correlation plane with the MOSLM used as the input device.

NOTE: Central DC area is partially blocked and the starburst pattern is due to an iris introduced in the addressing arrangement.

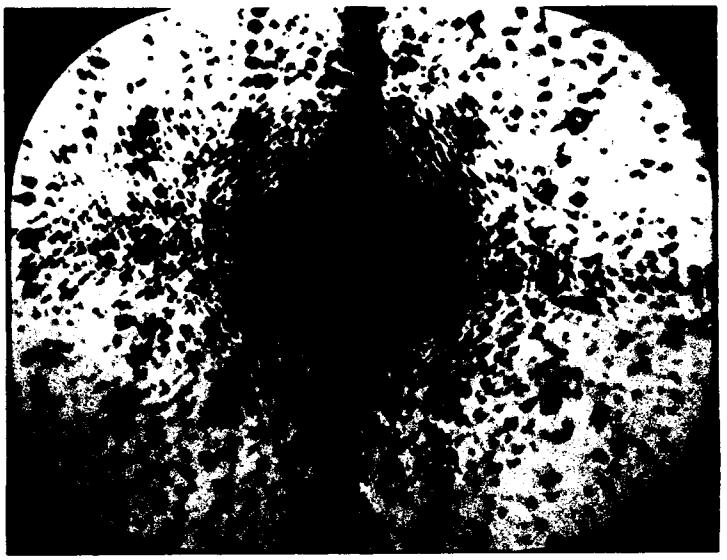

Figure 17. Fringe structure of the photographic recording (50x magnification).

0.1 percent of the energy incident on the plate was diffracted into each of the cross-correlation terms. A rotation of one of the tanks was then performed with respect to the other (Fig. 15) and another plate exposed, developed, and addressed using the same procedure. No correlation terms were observed. This is what would normally be expected with a Vander Lugt matched filter.

The polarizer was then rotated for phase modulation of the images displayed on the MOSLM device, and an identical sequence of exposures was performed. The correlations achieved by this method were little different than those fabricated with the MOSLM in the amplitude mode. Translational invariance was again proven to be correct with this correlator architecture and, as expected, no correlation occurred when one tank was significantly rotated with respect to the other.

The primary reason for these correlations being merely adequate is the fact that the MOSLM, which is operated in a transmission mode, transmits only two percent of the light incident on its semiconductor chip. The exposures discussed above were also long in duration and probably allowed the interference fringes to drift. Although time did not permit, an interesting extension of this experiment would be the replacement of the 35 mW Helium-Neon laser, used in the optical setup shown in Figure 12, with a more powerful source such as an Argon laser.

V. THE USE OF A LIQUID CRYSTAL LIGHT VALVE AS A SQUARE-LAW DETECTOR IN A JOINT TRANSFORM CORRELATOR

For many practical applications, the joint transform correlator must have a real-time input device and a real-time square-law detector. The input device must be capable of providing a scene and a reference object at near real-time or video frame rates. Furthermore, the real-time square-law detector must be able to resolve the interference between the Fourier transforms of the scene and reference information. As shown in Section IV of this report, a capable candidate for the real-time input device may be the magneto-optic spatial light modulator. A potential real-time square-law detector, namely, the liquid crystal light valve (LCLV) is discussed below.

It was experimentally determined in Section III (see Fig. 8) that the minimum resolution this device must have in order to resolve the interference pattern produced by the transparencies of the tanks is 20 lp/mm. Some of the better operating devices available are capable of this resolution but, typically, a resolution of 10 lp/mm is normally reported for the Hughes Corporation LCLV. The particular light valve used in this investigation to explore the possibility of real-time detection has been known to provide at least 20 lp/mm, depending on several driving parameters such as waveform, amplitude, and frequency of the driving signal. This light valve was placed in the optical architecture as shown in Figure 18.

The architecture of Figure 18 utilized the transparencies of the tanks as the scene and reference information. The transparencies were illuminated by a collimated plane wave beam from a Spectra-Physics Model 124B Helium-Neon laser. The modulated beam was then transformed by FTL_1 which had a focal

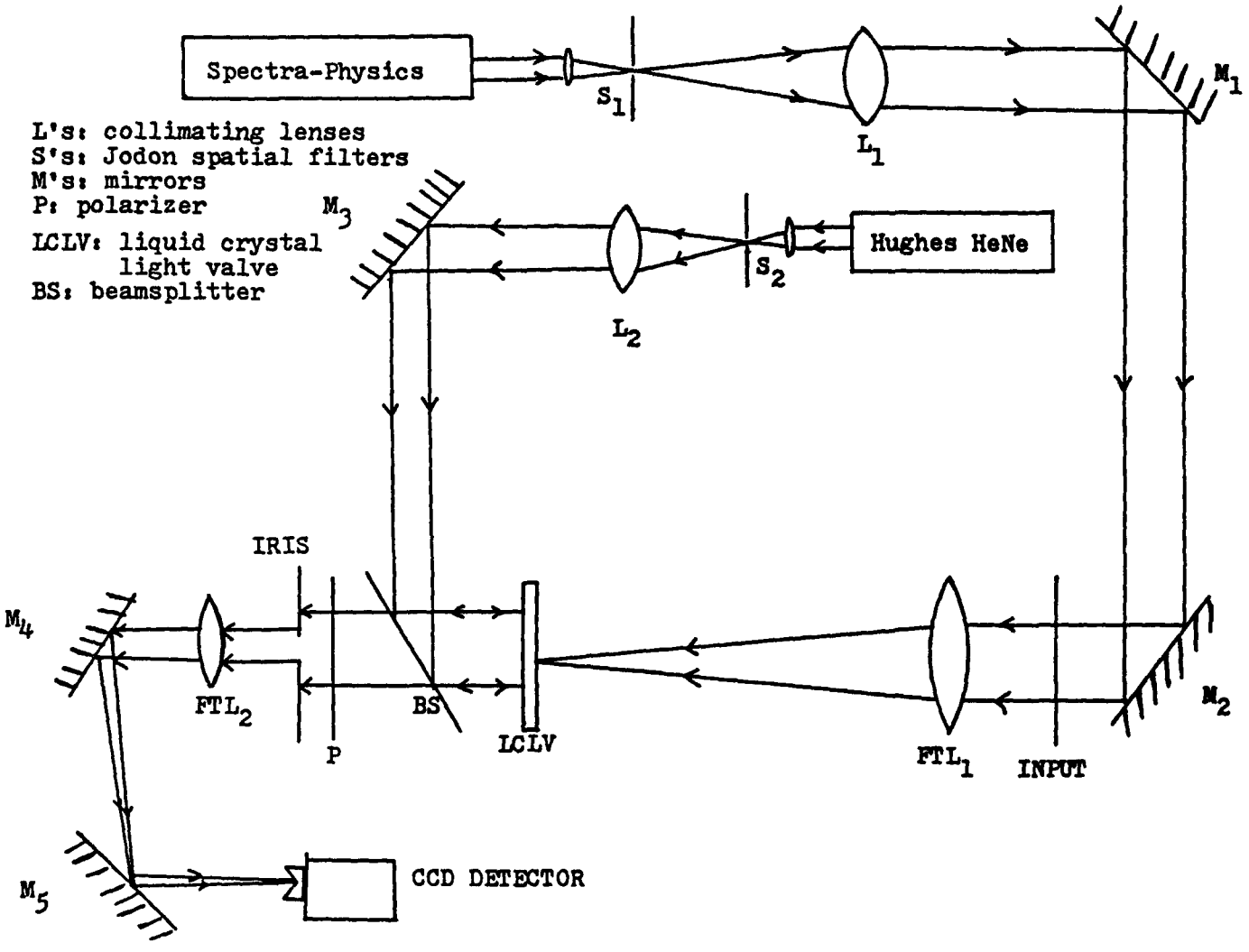

Figure 18. Experimental arrangement of a real-time JTC.

length of 1069 mm. At the transform plane, the light valve was introduced. The read side of the light valve was illuminated with a collimated plane wave provided by a Hughes 3221H-C HeNe laser. Upon reflection off of the light valve, the beam was directed through a polarizer for maximum contrast and an iris to block some unnecessary light information caused by multiple reflections from the beam splitter. The beam was then transformed using FTL_2 which had a focal length of 914 mm.

At the focal plane, no correlations were visible to the human eye; however, a camera was introduced into the focal plane and two faint but detectable cross-correlation signals were present. At this point, one of the tanks was physically blocked and the correlation signals were observed to disappear. This procedure, therefore, proves that a liquid crystal light valve can work moderately as a square-law detector in a joint transform correlator. However, for effective real world applications of a JTC, the resolution of the light valve, and spatial light modulators in general, must be improved beyond the current state of the art.

VI. CONCLUSION

The Joint Transform Correlator (JTC) is a viable alternative to the classical Vander Lugt matched filtering architecture due to the potential real-time correlating capability between a scene and a reference image. The efficiency of the JTC has been proven in some circumstances to be greater than that of a Vander Lugt system and the critical alignment of a matched filter is no longer a necessity.

The input information used in this investigation was provided by transparencies and later by a magneto-optic spatial light modulator. Future input devices, such as the recently developed deformable mirror device spatial light modulator from Texas Instruments or the amorphous silicon modulator reported by Ashley and Davis[17], could prove to be potentially significant improvements over these two methods of providing input information to the system.

Throughout this report, the resolution of the square-law detector was observed to be a major limitation of the joint transform architecture. However, great emphasis is currently being given to improving the resolution, as well as the response time, of spatial light modulators currently marketed. If these devices are improved, then the joint transform correlator could be a promising alternative to the Vander Lugt system.

REFERENCES

1. Vander Lugt, A., IEEE Transactions on Information Theory IT-10 (1964) : 139-145.

2. Duthie, J. G., and Upatnieks, J., Optical Engineering 23 (1984): 007.

3. Gregory, D. A., and Hudson, T. D., "Real-Time Pattern Recognition Using a Modified Liquid Crystal Television in a Coherent Optical Correlator," Technical Report RD-RE-86-1, MICOM, Redstone Arsenal, AL (1985).

4. Liu, H. K., Davis, J. A., and Lilly, R. A., Optics Letter 10 (1985) : 635.

5. Weaver, C. S., and Goodman, J. W., Applied Optics 5 (1966):1248-1249.

6. Casasent, D., "Pattern and Character Recognition," Handbook of Optical Holography, ed. H. J. Caulfield (New York : Academic Press, 1979), pp. 512-515.

7. Yu, F. T. S., Jutamulia, S., Lin, T. W., and Gregory, D. A., Applied Optics 26 (1987):1370-1372.

8. Yu, F. T. S., and Ludman, J. E., Optics Letter 11 (1986):395.

9. Rau, J. E., Journal of the Optical Society of America 57 (1967):798.

10. Ingwall, R. T., and Fielding, H. L., Optical Engineering 24 (1985):808.

11. Nisenson, P., and Sprague, R. A., Applied Optics 14 (1975):2602-2606.

12. Casasent, D., "Pattern and Character Recognition," Handbook of Optical Holography, ed. H.J. Caulfield (New York: Academic Press, 1979), pp. 512-513.

13. Rau, J. E., Journal of the Optical Society of America 57 (1967):800.

14. Casasent, D., and Furman, A., Applied Optics 16 (1977):285-286.

15. Shulman, A., Optical Data Processing (New York: Wiley, 1970), p. 560.

16. Lanteigne, D. J., and Hudson, T. D., "Fast Microcomputer Control of a Magneto-Optic Spatial Light Modulator," Technical Report RD-RE-86-10, MICOM, Redstone Arsenal, AL (1986).

17. Ashley, P. R., and Davis, J. H., Applied Optics 26 (1987):241-246.

DISTRIBUTION

	No. of Copies
Director US Army Research Office SLCRO-PH PO Box 12211 Research Triangle Park, NC 27709-2211	1
Director US Army Research Office SLCRO-ZC PO Box 12211 Research Triangle Park, NC 27709-2211	1
Headquarters Department of the Army DAMA-ARR Washington, DC 20310-0632	1
Headquarters OUSDR&E ATTN: Dr. Ted Berlincourt The Pentagon Washington, DC 20310-0632	1
Defense Advanced Research Projects Agency Defense Sciences Office Electronics Systems Division ATTN: Dr. John Neff 1400 Wilson Boulevard Arlington, VA 22209	1
Commander US Army Foreign Science and Technology Center AIAST-RA 220 Seventh Street NE Charlottesville, VA 22901-5396	1
Commander US Army Strategic Defense Command DASD-H-V PO Box 1500 Huntsville, AL 35807-3801	1
Director, URI University of Rochester College of Engineering and Applied Science The Institute of Optics Rochester, NY 14627	1

Director, JSOP
University of Arizona 1
Optical Science Center
Tucson, AZ 85721

Dr. Steve Butler 1
Electro-Optical Terminal Guidance Branch
Armament Laboratory
Eglin Air Force Base, FL 32542

Dr. Richard Munis 1
US Army
CRREL
72 Lyme Mill Rd.
Hanover, NJ 03755

Mark Norton
AMSEL-NV-T
Night Vision and Electro-Optics Center 1
Bldg 357
Fort Belvoir, VA 22060

Dr. Joseph Horner
RADC/ESOP 1
Hanscom AFB, MA 01731

Robert D. Buzzard
Applied Science Division
Applied Optics Operations 1
PO Box 3115
Garden Grove, CA 92641

Dr. J. W. Goodman
Department of Electrical Engineering 1
Stanford University
Stanford, CA 94305

Dr. H. John Caulfield 1
University of Alabama in Huntsville
Center for Applied Optics
Huntsville, AL 35899

Dr. J. G. Duthie
University of Alabama in Huntsville 1
Physics Department
Huntsville, AL 35899

Dr. David Casasent
Carnegie-Mellon University
Department of Electrical and Computer Engineering 1
Pittsburgh, PA 15213

Dr. F. T. S. Yu Penn State University Department of Electrical Engineering University Park, PA 16802	1
James F. Hawk University of Alabama in Birmingham Physics Department University Station Birmingham, AL 35294	1
Dr. Richard Juday NASA Johnson Space Center Code EE-6 Houston, TX 77058	1
Dr. Robert Kallman North Texas State University Mathematics Department Denton, TX 76203	1
H. K. Liu Jet Propulsion Lab 4800 Oak Grove Drive Pasadena, CA 91109	1
IIT Research Institute ATTN: GACIAC 10 W. 35th Street Chicago, IL 60616	1
US Army Materiel System Analysis Activity ATTN: AMXSY-MP Aberdeen Proving Ground, MD 21005	1
AMSMI-RD, Dr. McCorkle	1
Dr. Rhoades	1
AMSMI-RD-RE, Dr. R. Hartman	1
Dr. J. Bennett	1
AMSMI-RD-RE-OP, Dr. Don A. Gregory	1
Mr. David J. Lanteigne	1
Mr. James C. Kirsch	1
Mr. Tracy D. Hudson	80
AMSMI-RD-CS-R	15
AMSMI-RD-CS-T	1
AMSMI-GC-IP, Mr. Bush	1
AMSMI-RD-AS-OG, Ray Farmer	1